Rotating-Disk Dissolution Kinetics of Nitrofurantoin Anhydrate and Monohydrate at Various Temperatures

Makoto Otsuka,[1,2] Reiko Teraoka,[1] and Yoshihisa Matsuda[1]

Received November 9, 1990; accepted August 21, 1991

The dissolution behavior of nitrofurantoin anhydrate and monohydrate in JP XI, second fluid (pH 6.8) was investigated at various temperatures using a dispersed-amount method and a rotating-disk method. The initial dissolution process of the monohydrate obtained by the rotating-disk method followed the Noyes–Whitney–Nernst equation, but that of the anhydrate did not. The initial dissolution process of the anhydrate was analyzed by a dissolution kinetics equation involving the phase transformation process from anhydrate to monohydrate. The maximal concentration, the dissolution rate constant, and the rate constant of the phase transition process were estimated. The thermodynamic parameters for the dissolution processes of the anhydrate and monohydrate were obtained from van't Hoff plots and Arrhenius plots, respectively. The results of the intrinsic solubility and dissolution parameters of anhydrate and monohydrate suggest the possibility that the difference in the dissolution rates of the anhydrate and monohydrate affect the bioavailability of nitrofurantoin preparation. Information on the dissolution behavior of nitrofurantoin pseudopolymorphs is therefore useful for designing high-quality preparations.

KEY WORDS: nitrofurantoin; anhydrate; monohydrate; dissolution; rotating disk.

INTRODUCTION

The absorption rate of a drug administered orally is controlled by many factors, among which the dissolution rate is the most important (1). Nitrofurantoin (2), which is widely used as a urinary tract antibacterial drug, has a variable bioavailability (3–5), and its formulation factors, mainly particle size (6), affect the dissolution rate and thus the bioavailability in humans and the incidence of side effects (7). Therefore, the USP XXII (1990) monograph for nitrofurantoin tablets requires that not less than 25% of the labeled amount of drug be dissolved in 60 min in pH 7.2 phosphate buffer. The characterization of nitrofurantoin anhydrate and monohydrate was reported by Marshall and York (8), however, without analysis of the dissolution behavior. We reported that the apparent solubility of the anhydrate at 37°C in buffer solution at pH 6.8 (JP XI, second fluid) was 1.44 times higher than that of the monohydrate using the dispersed-amount method (9). However, it was difficult to estimate the intrinsic solubility of the anhydrate because the anhydrate transformed into the monohydrate before the concentration of the drug dissolved reached the equilibrium solubility. Therefore, the dissolution behaviors and solubilities of the anhydrate and monohydrate of the drug in buffer solution at pH 6.8 (JP, XI, second fluid) were evaluated in the present study using a rotating-disk method based on the dissolution kinetic model.

[1] Department of Pharmaceutical Technology, Kobe Women's College of Pharmacy, Motoyama-Kitamachi 4-19-1, Higashi-Nada, Kobe 658, Japan.

[2] To whom correspondence should be addressed.

MATERIALS AND METHODS

Materials. Nitrofurantoin powder (Lot No. 11085) was obtained from Fukujyu Pharmaceutical Co. Ltd., Japan. The preparation methods of the anhydrate and monohydrate were as reported previously (9). The pellets for the rotating-disk method were prepared by the following method: a 300-mg sample of powder was compressed in a cylindrical die of 1.5-cm diameter at a compression speed of 1.3 cm/min at 140 kg/cm^2 using an accurate compression/tension testing machine (Autograph Model IS-5000, Shimadzu Co.), and then the compressed pellet was kept for 5 min in the die at that compression pressure. The ejected pellet was fixed to a dissolution holder with bee wax so that only one side of the pellet surface was exposed.

X-Ray Powder Diffraction Analysis. X-ray powder diffraction profiles were taken at room temperature with an X-ray diffractometer (Type XD-3A, Shimadzu Co.). The operating conditions were as follows: target, Cu; filter, Ni; voltage, 20 kV; current, 5 mA; receiving slit, 0.1 mm; time constant, 1 s; counting range, 1 kcps; and scanning speed, 1° 2θ/min.

Dissolution Study Using the Dispersed Amount Method. The JP XI, second fluid (pH 6.8) was obtained as follows: 118 ml of 0.2 *N* NaOH solution was added to 250 ml of 2 *M* KH_2PO_4 solution, and the mixture diluted with water to 1000 ml. The dissolution profiles of the anhydrate and monohydrate were investigated in JP XI, second fluid. An excess amount (500 mg) of sample was introduced into 300 ml of dissolution medium in a 1000-ml round-bottomed flask with a plastic cover. The flask was fixed on the sample holder in a thermostatically regulated water bath maintained at 25, 30, 37, 40, and 45 ± 0.5°C and stirred by a paddle at 200 rpm. Aliquots (5 ml) of the solution were withdrawn at appropriate time intervals with a syringe through a 0.8-μm-membrane filter and diluted with the dissolution medium for spectrophotometric analysis (UV 160A, Shimadzu Co.) at 370 nm. The resultant loss in volume was compensated by adding the dissolution medium maintained at the same temperature.

Initial Dissolution Curve Measurement. The initial dissolution profiles of the anhydrate and monohydrate were investigated in JP XI, second fluid (pH 6.8) at 25, 30, 37, and 45 ± 0.5°C. The pellet fixed to the holder was set up on the dissolution instrument. The sample holder was rotated at 630 ± 5 rpm in 100 ml of dissolution medium in a 1000-ml round bottomed flask with a plastic cover. The solution was introduced into a quartz flow-through cell with a peristaltic pump and the concentration was determined spectrophotometrically at 370 nm.

Kinetic Interpretation of the Transformation of the Anhydrate to the Monohydrate During the Dissolution Pro-

0724-8741/92/0300-0307$06.50/0

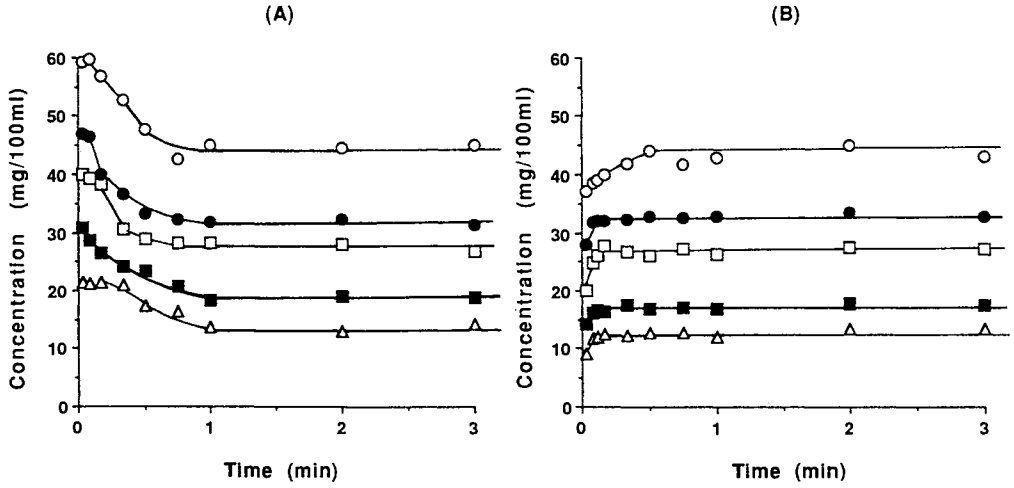

Fig. 1. Effect of temperature on the dissolution profiles of the anhydrate (A) and monohydrate (B) at pH 6.8 (JPXI, second fluid) by the dispersed-amount method. (△) 25°C; (■) 30°C; (□) 37°C; (●) 40°C; (○) 45°C.

cess. The initial dissolution curves of the anhydrate and monohydrate were determined according to the method described in the previous section. The computer program MULTI (10) was applied to perform nonlinear least-squares analysis of the dissolution kinetics equation. The kinetic parameters were calculated by using the damping Gauss–Newton method, after the initial values of the parameters were determined by the Simplex method. A weight of unity was employed in this analysis.

RESULTS AND DISCUSSION

X-Ray Powder Diffraction Analysis of the Anhydrate and Monohydrate

The anhydrate had the main diffraction peaks at 14.4 and 28.8° (2θ), while the monohydrate had peaks at 10.1, 12.3, 13.9, and 27.2°, indicating that both modifications are significantly different diffraction patterns, as reported in the previous papers (8,9). After compression at 140 kg/cm^2, the pellets of the anhydrate and monohydrate were carefully ground with an agate mortar and pestle, then X-ray powder diffraction profiles were recorded. The X-ray diffraction profiles of the compressed anhydrate and monohydrate were identical to those of the original samples for every crystal form. The results of the X-ray diffraction pattern suggest that no crystallographic change had occurred for these crystal forms during the compression process under the present experimental conditions.

Dissolution Profiles of the Anhydrate and Monohydrate Obtained by the Dispersed-Amount Method

Figure 1 shows the dissolution profiles of the anhydrate and monohydrate at various temperatures. The anhydrate showed characteristic convex dissolution curves with a maximal concentration at every temperature, whereas the monohydrate showed only normal dissolution curves. The dissolution curves of the anhydrate obtained by the dispersed-amount method were similar to those of theophylline involving a crystallization process together with a phase change from the anhydrate to monohydrate (11). After the dissolution experiment for the anhydrate, the X-ray powder diffraction patterns of crystallized precipitate coincided with those of the intact monohydrate. This result suggests that the dissolution behavior of the anhydrate involved a crystallization process together with a phase change from anhydrate to monohydrate. The solubilities of the monohydrate and the maximum concentration (apparent solubility) of the anhy-

Table I. Solubilities and Rate Constants of Phase Transformation and Dissolution Processes of the Anhydrate at Various Temperatures

Temperature (°C)	C_{sa}[a] ± SD (C_{sb})[e] (mg/100 ml)	C_{sh}[b] ± SD (mg/100 ml)	K_r[a] ± SD × 10^3 (sec^{-1})	K_t[c] ± SD × 10^5 (sec^{-1})	SS[d] × 10^3 (AIC)[f]
25	32.5 ± 0.4 (21.5)	13.2 ± 0.6	1.63 ± 0.07	5.45 ± 0.18	2.00 (−163)
30	40.1 ± 0.5 (30.5)	17.9 ± 0.4	1.88 ± 0.07	5.82 ± 0.20	3.65 (−148)
37	60.4 ± 0.8 (39.5)	27.4 ± 0.5	2.32 ± 0.08	6.73 ± 0.25	9.36 (−122)
45	86.3 ± 2.1 (60.0)	43.8 ± 0.8	2.83 ± 0.20	7.38 ± 0.18	60.9 (−71.5)

[a] The parameters were calculated by the MULTI program.
[b] Solubility was obtained by the dispersed amount method (n = 5).
[c] The values were calculated from the initial dissolution rate constant by the least-squares method (n = 3).
[d] The residual sum of squares.
[e] Apparent solubility (maximum concentration of dissolution profiles in Fig. 3).
[f] Akaike's information criterion.

drate are summarized in Table I, in which the apparent solubility was not the true value because the transformation rate of the anhydrate to the monohydrate was very high. It is therefore necessary to carry out dissolution kinetic experiments using the rotating-disk method when estimating the solubility of the anhydrate.

Dissolution Profiles of the Anhydrate and Monohydrate Obtained by the Rotating-Disk Method

Figure 2 shows the initial dissolution curves of the anhydrate and monohydrate at pH 6.8 and 37°C. The dissolution process of the monohydrate followed the Noyes–Whitney–Nernst equation, whereas that of the anhydrate did not. The slope of the dissolution curve of the anhydrate after the completion of the transformation accompanying crystallization was almost the same as that of the monohydrate. Nogami *et al.* (12) reported on the dissolution phenomena of *p*-hydroxybenzoic acid and phenobarbital involving a simultaneous phase change from anhydrate to hydrate. They considered the diffusion constant of the anhydrate to be almost the same as that of the hydrate and proposed the following equation for dissolution in the initial stage.

$$dC/dt = K_t \{C_{sa} \exp(-K_r t) + C_{sh} [1 - \exp(-K_r t)]\} \quad (1)$$

$$C = K_t (C_{sa} - C_{sh})[1 - \exp(-K_r t)]/K_r + K_r C_{sh} t \quad (2)$$

where C is the concentration of the drug in bulk solution, C_{sa} and C_{sh} are the solubilities of the anhydrate and monohydrate, respectively, t is time, K_t is the dissolution rate constant and K_r is the rate constant of the phase transformation process.

Since the dissolution process of the anhydrate of nitrofurantoin involved a phase change caused by hydration as shown in Fig. 3, and since one can assume that the diffusion constant of the anhydrate is the same as that of the monohydrate, the data were analyzed by Eq. (2), and the kinetic parameters in Eq. (1) were estimated. C_s was measured from the dispersed amount method and K_t was calculated from the initial dissolution rate of monohydrate, respectively. K_r and

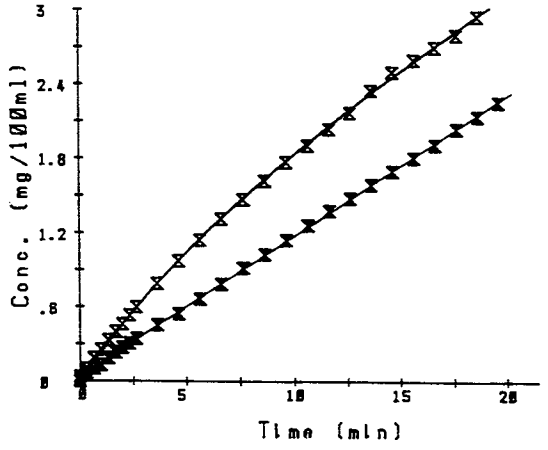

Fig. 2. Initial dissolution curves of the anhydrate and monohydrate at pH 6.8 at 37°C using the rotating-disk method. The open and filled symbols represent the anhydrate and monohydrate, respectively. The solid lines represent the theoretical values.

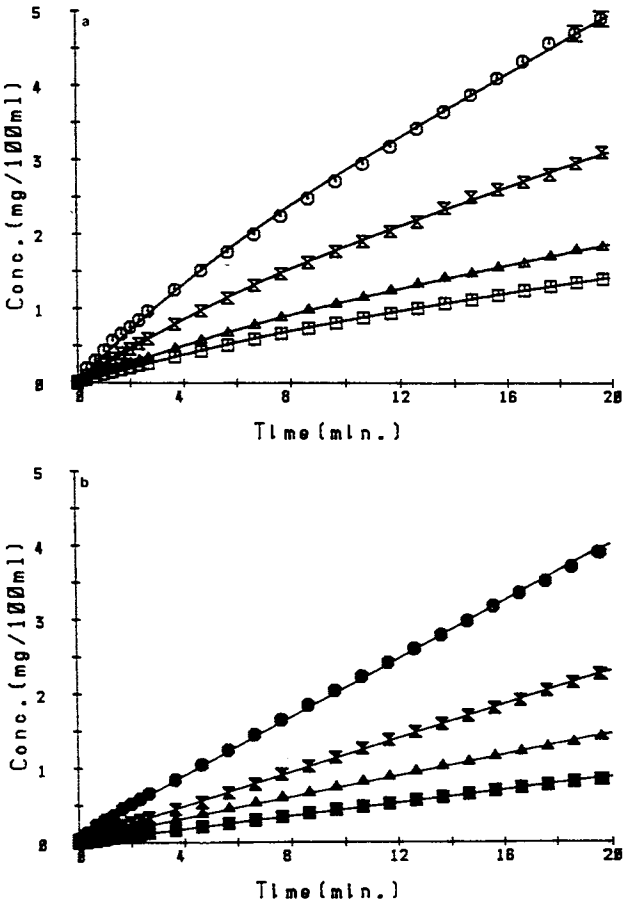

Fig. 3. Effect of temperature on the initial dissolution curves of the anhydrate (a) and monohydrate (b) at pH 6.8 using the rotating-disk method. (□, ■) 25°C; (△, ▲) 30°C; (⧗ , ⧗) 37°C; (○, ●) 45°C. The open and filled symbols represent the anhydrate and monohydrate, respectively. The solid lines represent the theoretical values.

C_a of nitrofurantoin were estimated using a nonlinear least-squares computer program MULTI (10). These parameters are given in Table I. The results of fitting the index parameter [the residual sum of squares (SS) and Akaike's informa-

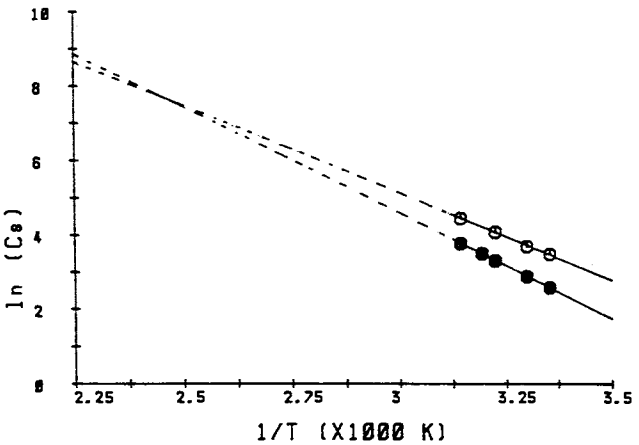

Fig. 4. The van't Hoff plot for the anhydrate and monohydrate at pH 6.8. The open and filled symbols represent the monohydrate and anhydrate, respectively.

Table II. Thermodynamic Parameters of the Anhydrate and Monohydrate at pH 6.8 (JP XI, Second Fluid)

Sample	Transition temperature (°C)	Heat of solution (kJ/mol)	Heat of transition (kJ/mol)	$\Delta G_{30°C}$ (kJ/mol)	$\Delta S_{30°C}$ (J/K)
NF					
Anhydrate	134 (125)[a]	39.1	−8.22	−2.03	−20.4
Monohydrate		47.3			
p-HA[b]					
Anhydrate	84	35.2	−5.4	—	−18.0
Hydrate		40.6			
PhB[c]					
Anhydrate	37	22.2	−8.9	—	−28.9
Hydrate		30.9			
CP[d]					
Form II	127	19.2	−9.96	—	−2.4
Form A		21.2			

[a] Dehydration temperature as measured with a DSC instrument (heating rate, 5°C/min).
[b] *p*-Hydroxybenzoic acid (Nogami *et al.*, 1969).
[c] Phenobarbital (Nogami *et al.*, 1969).
[d] Chlorpropamide (Ueda *et al.*, 1984).

tion criterion (AIC)] were satisfactory enough to support the belief that these equations might be applicable to the present dissolution process. The theoretical values (shown by the solid lines in Fig. 3) were in good agreement with the observed values under all dissolution conditions.

Effect of Temperature on the Dissolution Behavior

Figure 3 shows the effect of temperature on the initial dissolution curves of the anhydrate and monohydrate. The dissolution rates for the anhydrate after the phase change was completed were in good agreement with those obtained for the monohydrate at all temperatures. The kinetic parameters estimated by a nonlinear curve-fitting program are summarized in Table I. These values increased more or less with an elevation of temperature.

Figure 4 shows the van't Hoff plot for the anhydrate and monohydrate. These plots showed a linear relationship within the temperature range studied, indicating that the intersection of the extension of the two straight lines is at about 134°C. The heat of solution (Table II) was estimated from the slope of the line. The transition temperature of the anhydrate to the monohydrate was close to the dehydration temperature measured by a differential scanning calorimetry instrument. The heat of solution and the entropy change for the anhydrate and monohydrate were comparable to those obtained for other drugs (12–14). Since the side effects caused by fluctuations in the dissolution rate and the bioavailability of the commercial preparations of nitrofurantoin have been reported (7), the control of fluctuation of bioavailability is essential in practical therapy. Enhanced bioavailability by dosing the anhydrate is expected on the basis of the free energy difference (about 2kJ/mol) for the two modifications of nitrofurantoin (12–14).

Figure 5 shows the Arrhenius plot for phase transformation and dissolution processes of the anhydrate. The activation energies for both processes calculated from the slopes of the regression lines are summarized in Table III. The activation energy for the dissolution process of nitrofurantoin anhydrate was about three times larger than those reported for the dissolution process involving a phase change from anhydrate to hydrate for hydroxybenzoic acid or phenobarbital (12), and the value for the phase transformation process was 60% larger than those for hydroxybenzoic acid or phenobarbital.

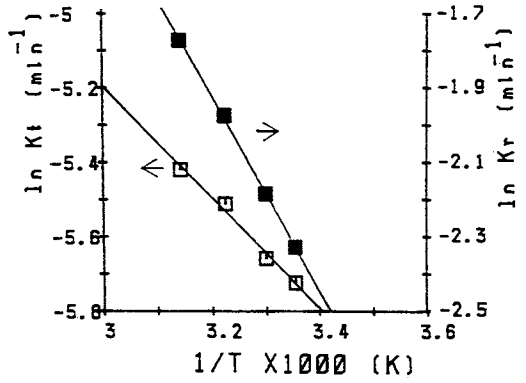

Fig. 5. Arrhenius plot for phase transformation and dissolution processes at pH 6.8. The open and filled symbols represent the dissolution and phase transformation processes, respectively.

Table III. Activation Energies (E) for Phase Transition and Dissolution Processes

Sample	E (kJ/mol)	
	Phase transformation	Dissolution
NF anhydrate	22.1	12.4
p-HA[a] anhydrate	14.1	3.49
PhB[b] anhydrate	9.99	3.63
CP[c] form II	13.7	3.89

[a] *p*-Hydroxybenzoic acid (Nogami *et al.*, 1969).
[b] Phenobarbital (Nogami *et al.*, 1969).
[c] Chlorpropamide (Ueda *et al.*, 1984).

ACKNOWLEDGMENT

The authors wish to express their gratitude to Miss Yuriko Arino for her assistance in the experimental work.

REFERENCES

1. L. Leeson and T. Carstensen. *Dissolution Technology*, American Pharmaceutical Association, Washington, D.C., 1974, Vol. 58, p. 145.
2. D. E. Cadwallader and H. W. Jun. Nitrofurantoin. *Anal. Profiles Drug Subst.* 3:346 (1976).
3. A. E. A. R. Ebian, R. M. A. Moustafa, and E. B. Abul-Enin. Nitrofurantoin. I. Effect of aging at different relative humidities and higher temperatures on the drug release and the physical properties of tablets. *Egypt. J. Pharm. Sci.* 26:287–300 (1985).
4. A. E. A. R. Ebian, H. T. Fikrat, R. M. A. Moustafa, and E. B. Abul-Enin. Nitrofurantoin. II. Correlation of in vivo bioavailability to in vitro dissolution of nitrofurantoin tablets aged at different relative humidities and elevated temperatures. *Egypt. J. Pharm. Sci.* 27:347–358 (1986).
5. H. W. Gouda, M. A.. Moustafa, and H. I. Al-Shora. Effect of storage on nitrofurantoin solid dosage forms. *Int. J. Pharm.* 18:213–215 (1984).
6. H. E. Paul, K. J. Hayes, M. F. Paul, and A. R. Borgmann. Laboratory studies with nitrofurantoin. Relationship between crystal size, urinary excretion in the rat and human, and emesis in dogs. *J. Pharm. Sci.* 56:882–885 (1967).
7. I. J. McGilveray, G. L. Mattok, and R. D. Hossie. The comparison of the bioavailabilities of commercial nitrofurantoin tablets. *Rev. Can. Biol.* 32:99–106 (1973).
8. P. V. Marshall and P. York. Crystallization solvent induced solid-state and particulate modifications of nitrofurantoin. *Int. J. Pharm.* 55:257–263 (1989).
9. M. Otsuka, R. Teraoka, and Y. Matsuda. Characterization of nitrofurantoin anhydrate and monohydrate, and their dissolution behaviors. *Chem. Pharm. Bull.* 38:833–835 (1990).
10. T. Yamaoka, Y. Tanigawara, T. Nakagawa, and T. Uno. A pharmacokinetic analysis program (MULTI) for microcomputer. *J. Pharmacobio-Dyn.* 4:879–885 (1981).
11. E. Shefter and T. Higuchi. Dissolution behavior of crystalline solvated and nonsolvated forms of some pharmaceuticals. *J. Pharm. Sci.* 52:781–791 (1963).
12. H. Nogami, T. Nagai, and T. Yotsuyanagi. Dissolution phenomena of organic medicinals involving simultaneous phase changes. *Chem. Pharm. Bull.* 17:499–509 (1969).
13. H. Nogami, T. Nagai, E. Fukuoka, and T. Yotsuyanagi. Dissolution kinetics of barbital polymorphs. *Chem Pharm. Bull.* 17:23–31 (1969).
14. H. Ueda, N. Nambu, and T. Nagai. Dissolution behavior of chlorpropamide polymorphs. *Chem. Pharm. Bull.* 32:244–250 (1984).